doi:10.1093/brain/awh645 *Brain* (2006), **129,** 189–199

Apoptosis dominant in the periinfarct area of human ischaemic stroke—a possible target of antiapoptotic treatments

Tiina Sairanen,[1,2] Marja-Liisa Karjalainen-Lindsberg,[1,3] Anders Paetau,[3] Petra Ijäs[1,2] and Perttu J. Lindsberg[1,2]

[1]Neuroscience Program, Biomedicum Helsinki, [2]Departments of Neurology and [3]Pathology, Helsinki University Central Hospital, University of Helsinki, Helsinki, Finland

*Correspondence to: Dr Tiina Sairanen, Department of Neurology, Helsinki University Central Hospital, PB 340, FIN-00029 HUS, Helsinki, Finland
E-mail: tiina.sairanen@hus.fi

Animal experiments have suggested that apoptotic programmed cell death is responsible for an important portion of the delayed ischaemic brain damage. Antiapoptotic signalling through erythropoietin (EPO) binding to its receptor (EPOR) is triggered by systemic or local hypoxia and may exist in the post-ischaemic brain, and a neuroprotective effect by EPO was described recently and proposed for clinical stroke treatment. The objective of the study was to determine whether apoptosis occurs in human ischaemic stroke and to describe its topographical distribution. An autopsy cohort consisting of 13 cases of fatal ischaemic stroke (symptom duration from 15 h to 18 days) treated at the Department of Neurology, Helsinki University Central Hospital and 3 controls were studied. DNA damage was investigated by immunofluorescent TUNEL-labelling in combination with apoptotic cell morphology and by visualization of a major signalling system of apoptosis, Fas–FasL (Fas-ligand), by the immunoperoxidase technique. The relationship of EPO and EPOR in the face of TUNEL-labelled and necrotic cell death was co-registered in human cerebral neurons undergoing different stages of ischaemic change. TUNEL-labelled cells with apoptotic morphology were disproportionately more frequent, 148% (30) [mean (SE)] in the periinfarct versus 97% (22) in the core, as percentage of the cells in the contralateral hemisphere ($P = 0.027$). The apoptotic cell percentage reached up to 26% (2) of all cells in periinfarct area. A linear correlation was found for Fas and its counterpart FasL expression ($r_S = 0.774$, $P < 0.001$). Ischaemia induced widespread neuronal expression of EPOR, which was inversely related to the severity of ischaemic neuronal necrosis ($P < 0.05$). To conclude, these data verify the predominance of apoptosis in the periphery of human ischaemic infarctions. Fas and FasL were linearly overexpressed supporting that this 'death-receptor' complex may promote the completion of cell death. Increased EPO signalling may be a cellular response for survival in less severely damaged areas. These results support antiapoptotic therapies against delayed neuronal cell death in human ischaemic stroke.

Keywords: apoptosis; ischaemic stroke; human; pathophysiology; immunohistochemistry

Abbreviations: Ab = antibody; DAPI = 4′,6-diamino-2-phenylindole; EPO = erythropoietin; EPOR = erythropoietin receptor; FasL = Fas ligand; GFAP = astrocyte marker glial fibrillary acidic protein; MoAb = monoclonal antibody; NF-200 = neurofilament-200 kDa; Pc = polyclonal antibody; TUNEL = terminal deoxynucleotidyl transferase (TdT)-mediated dUTP nick end labelling

Received April 25, 2005. Revised August 17, 2005. Accepted August 30, 2005. Advance Access publication November 4, 2005

Introduction

It has recently been hypothesized based on animal experiments that apoptosis is responsible for an important portion of ischaemic brain damage, and that inhibitors of this cascade would harbour therapeutic, neuroprotective potential (Nicotera and Lipton, 1999). Apoptosis and necrosis are suggested to be the two poles of a continuum of cellular death

after ischaemic stroke (McManus and Buchan, 2000). Fas-ligand (FasL) and erythropoietin (EPO) have opposing effects on apoptosis and inflammatory reactions. In addition to inducing apoptosis, FasL can trigger secretion of pro-inflammatory cytokines, e.g. interleukin-1beta (IL-1β) through interleukin-1 converting enzyme (ICE) i.e. caspase-1 activity. Thus, caspases provide a straight-forward link between FasL-induced apoptosis and inflammation (O'Connell *et al.*, 2001). On the other hand, anti-inflammatory and antiapoptotic actions are one proposed mechanism of EPO-function in central nervous system (CNS) injury, including experimental brain ischaemia (Siren *et al.*, 2001) and autoimmune encephalomyelitis (Agnello *et al.*, 2002).

Cerebral expression of EPO and its receptor (EPOR) is induced by hypoxia (Digicaylioglu *et al.*, 1995; Bernaudin *et al.*, 1999). *In vitro*, a potent neuroprotective effect of EPO has been described (Morishita *et al.*, 1997) and, promisingly, reduction of ischaemic neuronal damage and neurological dysfunction by EPO has been shown in rodent models of brain ischaemia (Sadamoto *et al.*, 1998). In addition, administration of soluble (extracellular domain) EPOR, which neutralizes the brain-derived EPO, exacerbates ischaemic injury (Sakanaka *et al.*, 1998). This supports the idea that endogenous neuroprotection is mediated by EPO–EPOR signalling in experimental brain ischaemia (Sakanaka *et al.*, 1998). EPO is synthesized in response to hypoxic conditions through hypoxia-inducible factor 1alpha (HIF-1α), which reorients energy metabolism towards survival during hypoxia, hypoglycaemia and oxidative stress (Semenza and Wang, 1992). The net effect of EPO on erythroblasts is achieved through inhibition of apoptosis, and through promotion of cell proliferation and differentiation (Yoshimura and Misawa, 1998). It is intriguing that in a similar fashion EPO protects, by precluding the apoptotic pathway also in neurons, the cells most sensitive to experimental hypoxic damage (Siren *et al.*, 2001). EPO-signalling activates intracellular JAK/STAT (Janus-tyrosine kinase/signal transduction and activators of transcription) pathway that has been described to lead to proliferation of a certain type of CNS progenitor cells (Cattaneo *et al.*, 1996). EPO has also been suggested to have a role in brain development (Moritz *et al.*, 1997). These data suggest that EPO exerts a profound influence on intracellular signalling, both during development and in cerebral metabolic stress.

Failures in translating experimental breakthroughs into clinical success have occurred repeatedly in stroke research. We have previously demonstrated that molecular targets of putative neuroprotective regimen evolve and distribute dissimilarly in infarcted human and rodent brains (Sairanen *et al.*, 1998, 2001). Although antiapoptotic therapies are widely held a promising avenue in preventing ischaemic brain damage, the localization and distribution of apoptosis in the course of human stroke has been investigated only in a few prior studies (Guglielmo *et al.*, 1998; Love *et al.*, 2000). Our aim was to test whether apoptosis occurs in human ischaemic stroke and, if present, whether it localizes in the zone of rescuable tissue surrounding the rapidly lost infarct core.

EPO, on the other hand, has recently been viewed a promising neuroprotective, antiapoptotic substance (Siren *et al.*, 2001), and has also been already used clinically in human stroke patients to prevent brain damage (Ehrenreich *et al.*, 2002). Very little is known about the behaviour of this intriguing signalling system in human cerebral ischaemia. This led us to investigate the apoptosis and EPO–EPOR signalling, a proposed rescue mechanism, in human victims of fatal acute ischaemic stroke. As a potential mechanism of apoptosis, we also investigated the expression of Fas, a member of the tumour necrosis factor (TNF) superfamily of cell death receptors, and FasL, the overexpression of which leads to uncontrolled apoptosis (Sharma *et al.*, 2000).

Materials and methods

Autopsy material

We studied autopsy specimens from 13 cases of fatal ischaemic stroke (symptom duration from 15 h to 18 days) treated at the Department of Neurology, Helsinki University Central Hospital. Autopsies were performed within a mean of 18 h after death (range, 3.5–40 h). Three patients who died of a non-neurological cause served as controls (autopsy delays of 14, 14.5 and 21 h). The study protocol was approved by the institutional review committee of the Helsinki University Central Hospital. Informed consent was given by the relatives. Clinical characteristics are outlined in Table 1. Spontaneous, complete recanalization was not found in any of the cases. One patient received 1.1 mg/kg of alteplase (rt-PA) according to the European Cooperative Acute Stroke Study (ECASS) trial protocol, but no recanalization was achieved (Case 3; Table 1).

Neuropathology

Tissue sampling was based on individual infarct topography, which in each case was determined on the basis of cerebrovascular anatomy and the most recent CT scan. On autopsy, brain areas with variable degree of infarction were identified macroscopically and ~1 cm^3 cortical samples, including subcortical white matter, were dissected and fixed with formalin prior to embedding in paraffin or frozen at −70°C until analysed, as described previously (Lindsberg *et al.*, 1996). Samples from corresponding areas of the contralateral or non-infarcted hemispheres and from the control brains were processed in a similar way (Fig. 1).

The infarct maturation stage was scored in each tissue block based on standard histological signs of the severity of ischaemic neuronal necrosis (later referred as necrosis score). An experienced neuropathologist unaware of the patient history or the sample localization performed the scoring from standard haematoxylin–eosin stainings. Focusing on the integrity of the nucleus, scores for signs of ischaemic neuronal necrosis in each tissue section were as follows: Score 0, normal morphology represented by sharply delineated nuclei that can be differentiated from surrounding cytoplasm; Score 1, largely normal morphology but scattered neurons with nuclear abnormalities, such as pyknosis, low nuclear cytoplasmic contrast and smearing of nuclear border (similar to type III neurons by Eke *et al.*, 1990); Score 2, large proportion of neurons with nuclear abnormalities as mentioned for Score 1; Score 3, large proportion of neurons with nuclear abnormalities, with scattered ones exhibiting signs of irreversible damage, such as shrunken cytoplasm with irregular borders and invisible nuclei (similar to type IV neurons by Eke *et al.*, 1990);

Table 1 Characteristics of deceased stroke patients and controls studied post mortem

Case no[a]/gender	Age (years)	Risk factors[b]	Cause of death[c]	Survival time (days)	Occluded vessel[d]/HT[e]	Medication prior/ in-hospital[f]
1/M	63	AF, AS, DM, H, HF	VF, stroke	0.6	ICA/TE	ASA/—
2/F	89	AF, CAD, DM, H	Stroke	1	MCA/E HT	ASA/—
3/F	75	H	Herniation	1.2	MCA/T Ht	—/heparin, altepl.
4/F	67	CAD, HC, IE	Herniation	1.6	MCA/TE Ht	ASA/NSAID
5/F	44	None	Herniation	1.6	MCA/TE	—/—
6/M	82	None	Herniation	2.5	ICA/T	—/NSAID, heparin
7/M	74	AS, CAD	Stroke	2.5	BA/T HT	ASA/—
8/F	79	CAD, H, HF	PE (AMI, VF), stroke	3	MCA/T	—/—
9/F	72	AS (EA), CAD	Herniation	3	MCA/T	ASA/NSAID, heparin
10/M	48	HC	Stroke	5.4	MCA/T	ASA/—
11/F	65	CAD, H, HF	Stroke	8.5	BA/T	ASA, NSAID/heparin
12/F	75	AF, AS, CAD, DM, H	PE, stroke	17	ICA/T Ht	—/heparin, warfarin
13/M	79	AF, CAD, H, HF	PE, stroke	18	MCA/TE HT	NSAID/—
A/M	61	DM, H, HF	CA	—	—	NA
B/M	41	CAD	Duodenal ulcer	—	—	NA
C/M	60	AS, CAD, HF, IE	AMI	—	—	NA

[a]Cases A, B and C, control patients dying suddenly without a neurological cause. [b]Abbreviations for risk factors: AF = atrial fibrillation, AS = generalized arteriosclerosis, CAD = coronary artery disease, DM = diabetes mellitus, EA = carotid endarterectomy, H = hypertension, HC = hypercholesterolaemia, HF = heart failure and IE = chronic ischaemic encephalopathy. [c]Abbreviations for cause of death: VF = ventricular fibrillation, herniation = herniations of brain, CA = cardiac arrest, AMI = acute myocardial infarction and PE = pulmonary embolism. Immediate cause of death is given as first and contributing cause as second. [d]Abbreviations for occluded vessels: ICA = internal carotid artery, MCA = middle cerebral artery, BA = basilar artery, T = thrombosis and TE = thromboembolism. [e]HT = haemorraghic transformation according to neuropathology report, with HT referring to dense multifocal haemorraghes and more subtle, local haemorrhages denoted by ht. [f]Medications including acetylsalicylic acid (ASA) or non-steroidal anti-inflammatory drugs (NSAID) prior to hospitalization and in-hospital use of ASA, NSAIDs, thrombolytic agents (rt-PA; alteplase = altepl.), and/or anticoagulants including heparin or low molecular weight heparins (heparin) and warfarin. NA = not applicable.

and Score 4, large proportion of neurons with irreversible changes as mentioned for Score 3. In the topographical grouping of tissue blocks contralateral or control areas had ischaemic neuronal necrosis scores of 0 or 1, the periinfarct had scores from 1 to 3 and the infarct core had scores 3 or 4 (Fig. 1).

In situ cell death detection by TUNEL and triple-labelling immunofluorescent staining of TUNEL with FasL, EPO or EPOR, and DAPI

The TUNEL reaction (terminal deoxynucleotidyl transferase (TdT)-mediated dUTP nick end labelling) was carried out on paraffin-embedded sections according to manufacturer's instructions (*In situ* cell death detection kit, Fluorescein; Boehringer Mannheim GmbH). The washes included a rinse and two 5-min washes with phosphate buffered saline (PBS) between each step. The sections were mounted on cover slips with Vectashield-DAPI fluorescence mounting media containing 4′,6-diamino-2-phenylindole (Vector) and then investigated with an epifluorescence microscope (Zeiss Axiomat II). Omission of the TdT-enzyme abolished the TUNEL-signal (data not shown). Due to the scattered nature of apoptosis, cortical areas with maximal density/expression of TUNEL-positive cells with apoptotic nuclear changes were included in the statistical analysis. Ten fields with an area of 0.0935 mm^2 were counted from each brain location of all infarct cases. Intensively TUNEL-positive cells were defined apoptotic when they also showed apoptotic nuclear morphology (Fig. 2A–C). To rule out false TUNEL-positivity by endogenous nucleases, eight adjacent sections from periinfarct area, infarct core or contralateral hemisphere were either incubated in a 4% (v/v) ethanolic solution of diethyl pyrocarbonate (DEPC) for 30 min at 4°C before the microwave treatment (Stähelin *et al.*, 1998; Love *et al.*, 2000) or labelled without DEPC pretreatment. No decrease in the number of TUNEL-positive cells with apoptotic nuclear changes was evident with the pretreatment. Detection of FasL, EPO or EPOR was carried out as outlined below and was subsequently followed by the TUNEL reaction as described above.

Apoptotic DNA ladder assay

DNA extracted from brain tissue samples of Cases 4, 6 and 9 (Table 1) was analysed by agarose gel electrophoresis to detect apoptotic DNA fragmentation. In addition, samples from a control patient and from the frontal lobe of a basilar artery thrombosis patient (Case 7) were studied as controls. DNA was extracted by a method modified from Blin and Stafford (1976). Briefly, 500–1000 mg of frozen brain tissue was pulverized in liquid nitrogen and added to 10 volumes of lysis buffer [10 mM Tris–HCl (pH 8), 0.1 M EDTA (pH 8), 0.5% SDS and 20 μg/ml Rnase A]. The suspension was incubated at 37°C for 1 h after which 100 μg/ml of proteinase K was added and incubation was continued at 50°C overnight. The solution was extracted with

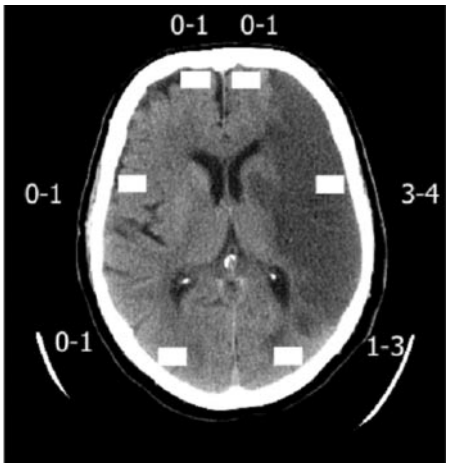

Fig. 1 Tissue sampling and histopathological scoring. Tissue sampling was based on the most recent CT-scan and 1 cm^3 cortical samples including subcortical white matter were dissected from the infarct core, periinfarct region and from non-ischaemic regions of the ipsilateral hemisphere. Samples from regions homologous to the above mentioned regions were obtained also from the contralateral hemisphere (white rectangles). Neuropathological scoring of the severity of nuclear ischaemic changes in neurons was done by an experienced neuropathologist unaware of the origin of the sample. In necrosis Score 0, neuronal morphology was normal; Score 1, most neurons normal; Score 2, some neurons with slight nuclear abnormality; Score 3, some neurons with irreversible damage; and Score 4, large proportion of neurons with irreversible changes (for detailed description see Materials and methods, Neuropathology). The samples from infarct core had ischaemia severity, with Scores 3 or 4. The samples from periinfarct regions had Scores 1–3. Samples from non-infarcted and from control brains had either Score 0 or 1.

phenol/chloroform/isoamyl alcohol, DNA was precipitated with 2 M ammonium acetate and 2 volumes of ethanol, and dissolved in TE buffer (10 mM Tris–HCl, 100 μM EDTA). A total of 7.5 μg of DNA was separated on a 1.5% agarose gel, stained with ethidium bromide (0.5 μg/ml) and visualized using ChemiDoc XR (BioRad).

Immunohistochemistry

The primary antibodies used in immunoperoxidase staining and in double-immunofluorescent labelling were as follows [antibody (Ab); dilution/incubation time (manufacturer)]: (i) Pc goat anti-human EPO (N-19:sc-1310); 1:50/overnight (Santa Cruz Biotechnology Inc., Santa Cruz, CA), (ii) goat immunoglobulin G (G IgG) as control for Ab # 1; 1:1250/overnight (Zymed Laboratories Inc., San Francisco, CA), (iii) Pc rabbit anti-human EPOR (M-20:sc-697); 1:500/overnight (Santa Cruz Biotechnology Inc.), (iv) Pc rabbit anti-human Fas (C-20:sc-715); 1:400/overnight (Santa Cruz Biotechnology Inc.), (v) Pc rabbit anti-human FasL (Q-20:sc-956); 1:100/overnight (Santa Cruz Biotechnology Inc.), (vi) rabbit immunoglobulin G (R IgG) as control for antibodies Ab # 3–5; 1:2500–1:12500/overnight (Vector Laboratories Inc., Burlingame, CA), (vii) MoAb mouse anti-neurofilament 200 kDa (NF-200); 1:50/1 h (Boehringer Mannheim, Indianapolis, IN), (viii) MoAb mouse anti-human glial fibrillary acidic protein (GFAP); 1:25/1 h (DAKO A/S, Glostrup, Denmark), and (ix) mouse immunoglobulin G_1 (m IgG_1) as control antibody for MoAbs # 7 and 8; 1:25/1 h, (DAKO A/S). (Abbreviations: Ab = antibody; Pc = polyclonal antibody and MoAb = monoclonal antibody.)

Paraffin-embedded sections were deparaffinized with xylene and hydrated through graded alcohols. Epitope unmasking by microwave irradiation in 0.1 M citrate buffer (pH 6.0) twice for 5 min at 800 W and once for 5 min at 600 W prior to cooling for 20 min was followed by quenching of the slides in 3% H_2O_2 in methanol. The slides assigned for erythropoietin staining were not irradiated and quenching was performed with 0.3% H_2O_2 in PBS. Blocking with 10% normal sera for 30 min prior to incubation with the primary antibody was followed by incubation with appropriate biotinylated secondary antibody (1:200) for 30 min and subsequent incubation with avidin–biotin complex for 40 min (Vectastain ABC Kit; Vector Laboratories Inc.). The horseradish peroxidase reaction was detected by incubation with chromogen diaminobenzidine (DAB) prior to counterstaining with Mayer's haemalum, according to manufacturer's instructions (SK-4100, Vector Laboratories Inc.).

Control experiments included the following steps:

(i) Inclusion of a positive tissue section:
  (a) In a second trimester placenta clear EPO immunostaining of the syncytiotrophoblast and cytotrophoblast cells as well as villous core cells was detected, consistent with the previous description (Conrad *et al.*, 1996).
  (b) In normal adult kidney, intense EPOR immunoreactivity was evident in tubular cells and in vascular structures, while the glomeruli were negative.
  (c) Fas and FasL immunoreactivity was evident in second trimester placenta.
(ii) Omission of the primary or secondary antibody abolished the immunoreactivities mentioned above.
(iii) Replacing the primary antibodies by non-immune immunoglobulin in equivalent concentration abolished specific staining and yielded only occasional background signal.
(iv) Preabsorption of the antibody with ×50 (weight) excess of accompanying control peptide (sc-1310 P; Santa Cruz) for EPO, EPOR (sc-697 P; Santa Cruz) and FasL (sc-956 P; Santa Cruz) antibodies, and with ×100 excess of peptide (sc-715 P; Santa Cruz) for Fas antibody prior to immunostaining abolished immunoreactivity (data not shown).

Double-labelling immunofluorescent staining

Epitope unmasking was performed by microwave irradiation in 0.1 M citrate buffer (pH 6.0) once for 5 min at 370 W followed by quick cooling with distilled water. The sections were then blocked with 3% bovine serum albumin (BSA) in 20% normal bovine serum/0.1 M Tris–HCl (pH 7.5) for 30 min. Overnight incubation with the primary antibody was succeeded by incubation with the appropriate secondary biotinylated antibody at 1:200 dilution for 30 min (Vector) and subsequent detection with Rhodamine Red®-conjugated Neutralite™ avidin (A6378; Molecular Probes Europe BV, The Netherlands) at 1:200 dilution for 30 min. Following these, cellular markers for neurofilaments (NF-200 kDa) and astrocytes (GFAP) were applied. These were visualized with the FITC-conjugated anti-mouse antibody (Dako A/S) at 1:20 dilution for 30 min.

Acquisition of microscopical data and statistical analyses

Based on our previous experience from this autopsy cohort (Lindsberg *et al.*, 1996), it can be shown that the culprit events

indicating infarct completion (ischaemic neuronal necrosis, neutrophil accumulation, macrophage accumulation) progress faster in the core and more slowly in the periphery of the infarct. Furthermore, unlike in studies of induced standard-sized infarcts in young experimental animals, our human brain material included spontaneous infarcts with variable duration and topography. We therefore determined the infarct maturation stage in each tissue block, based on the severity of ischaemic neuronal necrosis (Scores 0–4; Fig. 1). This also made sure that the ischaemic neuronal changes associated with secondary ischaemia, e.g. due to increased intracranial pressure, were represented as early ischaemic changes (i.e. infarct maturation Score 1) in the results. The present investigational microscopical data were then collected from the same tissue blocks from the infarct and periinfarct region and from homologous regions of the contralateral hemisphere. In each of these sections, immunoreactivity was evaluated in five randomly selected, consecutive fields of 0.3125 mm^2, resulting in a mean (SE) of immunopositive cell structures/mm^2. Furthermore, a semiquantitative grading of the intensity of the immunoreactive signal was performed.

The descriptive data are given as mean (SE). The difference between the mean numbers of immunoreactive cell structures/mm^2 in each brain location in the control brains and in post-ischaemic brains was evaluated by one-way ANOVA. The relative percentage of TUNEL-labelled apoptotic cells in infarct core and periinfarct areas within subjects was compared using paired *t*-test. Jonckheere–Terpstra trend test was applied to determine the strength of associations between the continuously distributed variables i.e. median immunoreactivities of EPO, EPOR, Fas, FasL or TUNEL-labelling and the class-ordered ischaemic neuronal necrosis, i.e. infarct maturation score. Spearman correlation coefficient (r_S) was used to assess the relation between Fas and FasL immunoreactive cells and Kendall's tau-b correlation coefficient in assessment of relation between EPOR immunoreactivity in somas and in cellular processes. In the box plots the median line is shown, the bar represents the upper 75% and lower 25% quartile, and the error bar depicts high and low values. Statistical analyses were performed using the SPSS for Windows program (version 10.07). A P-value < 0.05 was considered statistically significant.

Results

In situ cell death detection by TUNEL-labelling

In this autopsy cohort of infarcted human brains, DNA damage was detected by TUNEL-labelling and combined with light microsopical estimation of apoptotic nuclear morphology, supported by DNA fragmentation assay and immunohistochemical visualization of a major signalling system of apoptosis, Fas−FasL. Intensively TUNEL-positive cells were only defined apoptotic when they also showed apoptotic nuclear morphology (Fig. 2A–C) (Charriaut-Marlangue *et al.*, 1996). To concentrate on a potential therapeutic time window, the TUNEL-stainings were focused on cases with symptom durations up to 5.4 days ($n = 10$). In these brains of elderly individuals (mean age 67.1), TUNEL-labelled cells with apoptotic morphology were detected both ipsilaterally and contralaterally in the infarcted brains and also in control brains. However, a shift in the morphological appearance of TUNEL-positive cells was evident, so that the cells of the contralateral hemisphere showed only thickening of the nuclear envelope and condensation of the chromatin, with otherwise normal cellular morphology, whilst in transition to periinfarct and infarct core regions the morphological apoptotic changes were more advanced (Fig. 2A–C), as described by Charriaut-Marlangue *et al.* (1996).

TUNEL-labelled cells with morphological changes compatible with apoptosis dominated in the periinfarct area, since the relative proportion of TUNEL-labelled cells with apoptotic morphology as percentage of the contralateral hemisphere was 148% (30) in the periinfarct region and 97% (22) in the infarct core ($P = 0.027$) (Figs 3A, and 2D and E). In line, the percentage of TUNEL-labelled cells with apoptotic morphology tended to decrease as the ischaemic neuronal necrosis increased from Score 1 (the mildest ischaemic change) to 4 (irreversible ischaemic change in infarct core) ($P = 0.063$) (Fig. 3B). The mean percentage of TUNEL-labelled cells of the total DAPI-depicted cell number in brain areas with ischaemic neuronal necrosis Score 0 was 8% (2) (median 6; range 0–19%) (Fig. 3B).

Fas–FasL immunoreactivity

Most striking Fas and FasL immunoreactivity was seen in somas of cells determined morphologically as neurons by their large size, triangular nucleus and/or cytoplasm, distinct nucleolus and undivided, long cellular extension(s) (Fig. 2G). A closely correlated relation was evident between the numbers of Fas and FasL immunoreactive somas ($r_S = 0.774$, $P < 0.001$) (Fig. 3C). Similar to the TUNEL-labelled cell death, the number of FasL immunoreactive somas fell gradually in line with the increasing severity of ischaemic neuronal necrosis ($P = 0.013$), but was abundant also in normal regions (Fig. 3D).

Apoptotic DNA ladder assay

DNA ladder assay showed faint oligonucleosomal, apoptotic DNA fragmentation against random necrotic DNA degradation i.e. smear in ischaemic brain samples from two stroke patients (cases 6 and 9). DNA laddering was best visualized in Case 9, with symptom duration of 3 days (Fig. 4). The contralateral hemisphere also revealed faint laddering, but overall detection of laddering was obscured by the presence of concomitant necrotic DNA (Case 4; symptom duration 1.6 days, data not shown). Control samples displayed no DNA ladder and only negligible necrotic smear (Fig. 4); thus, it is shown that death-related or post-mortem processes do not cause laddering.

EPO and EPOR immunoreactivity

In all control brains ($n = 3$) some large cell somas and processes showed immunoreactivity for EPO. The post-ischaemic EPO immunoreactivity was most pronounced in these cellular extensions bilaterally. The neuronal origin of the immunoreactive signal was confirmed by a prominent overlap between

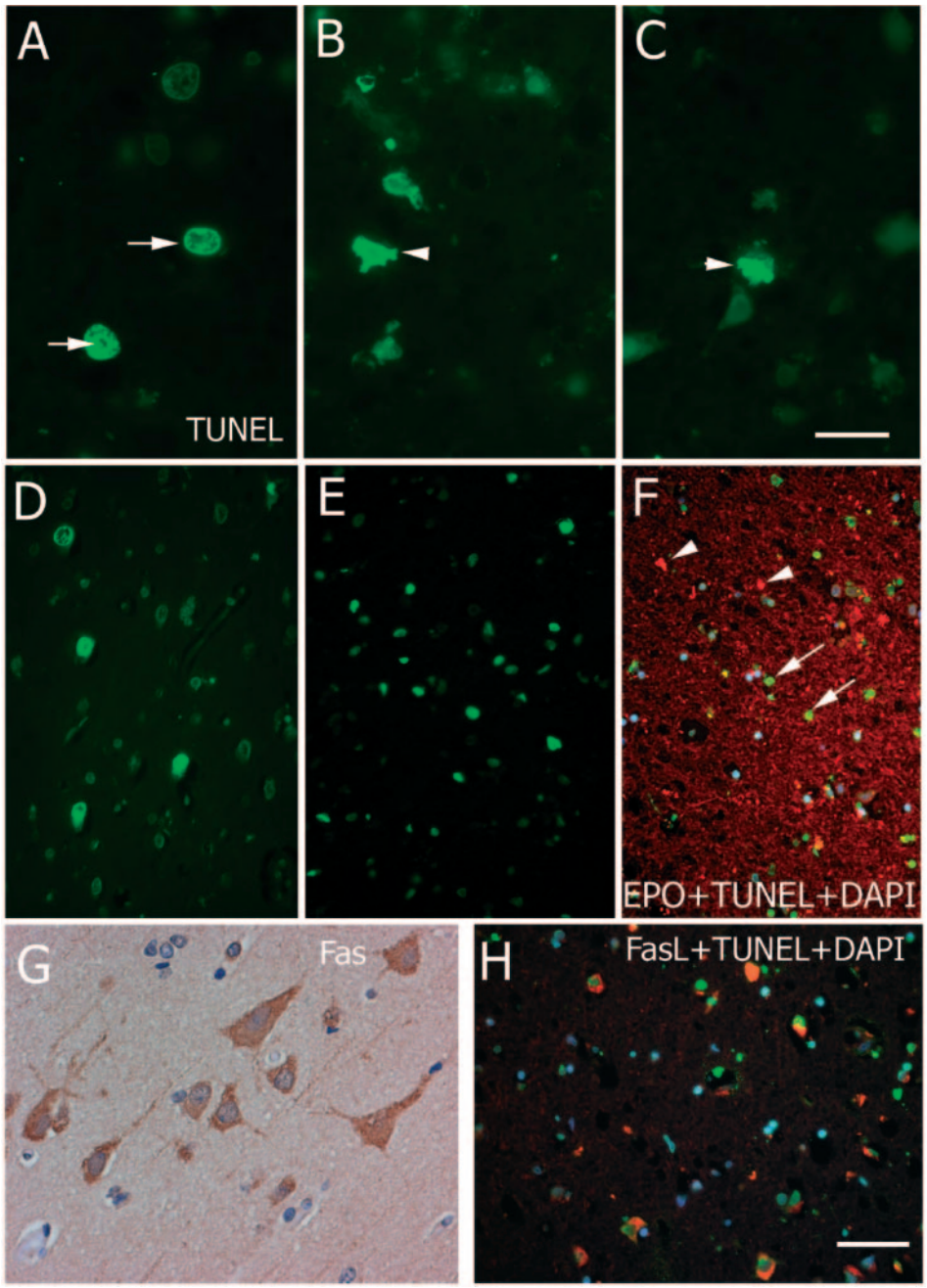

Fig. 2 TUNEL-labelled cell death (FITC in **A–F** and **H**), its co-localization with FasL (rhodamine in **H**), and dissociation of TUNEL-labelling and EPO (rhodamine in **F**) in ischaemic brains. TUNEL-labelled cells were named apoptotic when they showed simultaneously apoptotic nuclear changes at light microscopy. (**A**) A gradient in the nuclear apoptotic changes is evident. Scattered TUNEL-labelled cells with only thickened nuclear envelope and condensed chromatin (arrows) are dispersed among non-fluorescent cells, 0.6 day after thromboembolic ICA-occlusion. (**B**) Especially in the periinfarct region, many ipsilateral TUNEL-labelled cells started to lose the normal, rounded nuclear shape and had reduced cytoplasmic volume with convolution of cell membrane leading to blebbing (arrow head), 3 days after MCA-thrombosis. (**C**) In transition to the infarct core, many cells had lost nuclear contrast and showed further nuclear shrinkage (pyknosis) and on rare occasions showed formation of dense spheres i.e. apoptotic (arrow head), 3 days after MCA-thrombosis. (**D**) TUNEL-labelled cells with thickening of the nuclear envelope and condensation of the chromatin with otherwise normal cellular morphology were detected also contralaterally, 2.5 days after internal carotid artery occlusion. (**E**) TUNEL-labelled cells with apoptotic morphology were most abundant in the periinfarct region (for quantification see Fig. 3). (**F**) EPO immunofluorescence in large cell somas (arrow heads) most often dissociated from TUNEL-labelling (arrows), shown here from the infarction core (Case 4). (**G**) Fas and FasL immunoreactivity was most prominent in large cells with neuronal morphology. A peroxidase staining, with brownish Fas immunoreactivity, with haematoxylin counterstaining from periinfarct area, 3 days after MCA-thrombosis. (**H**) Post-ischaemic FasL immunoreactivity co-localized with TUNEL-labelling, shown here at infarction core 1.6 days after MCA-occlusion. The blue colour denotes DAPI-stained cell somas. Magnification is ×1300 in (A–C) and (G) (Scale bar = 10 μm), and ×300 in (D–F) and (H) (Scale bar = 40 μm).

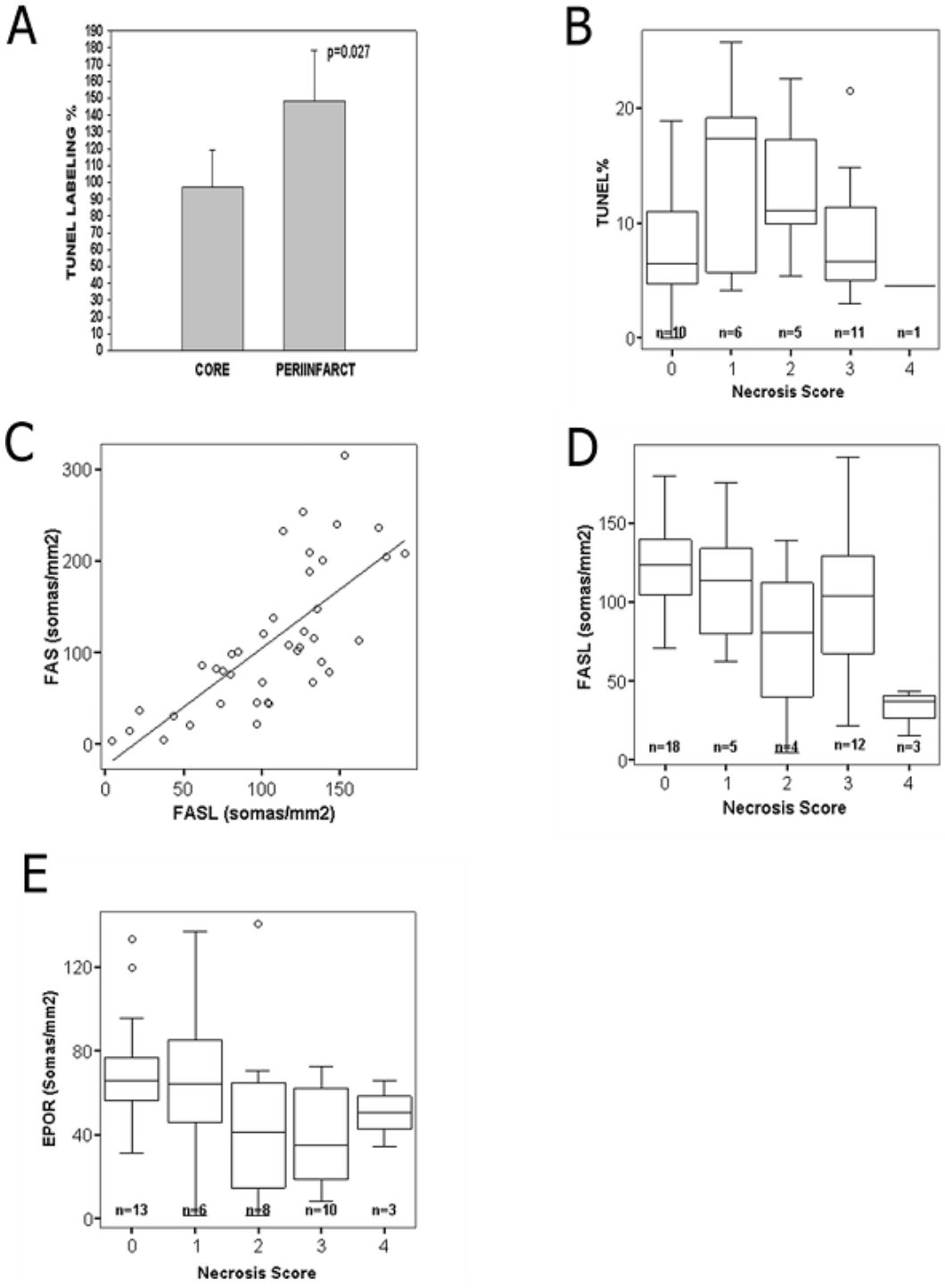

Fig. 3 (**A**) Percentage of TUNEL-labelling and (**B**) its correlation with ischaemic neuronal necrosis score. (**C**) Linear correlation between Fas and FasL immunoreactivity and (**D** and **E**) inverse relation of FasL and EPOR immunoreactivity with ischaemia severity. (A) TUNEL-labelled cells consistent with apoptotic morphology were disproportionately more frequent, 148% (30) [mean (SE)] in the periinfarct versus 97% (22) in the core area as percentage of the cells in the contralateral hemisphere ($P = 0.027$) between days 1 and 5 ($n = 10$). (B) A trend towards the highest percentage of TUNEL-labelled apoptotic cells in the brain area with the least ischaemic damage i.e. brain area with ischaemic neuronal necrosis Score 1 ($P = 0.063$). (C) Strong correlation between the Fas and FasL immunoreactive cell numbers in infarcted brains ($r_S = 0.774$, $P < 0.0001$). (D) Decline in the number of FasL immunoreactive cells along with increasing ischaemia severity ($P = 0.013$). (E) Inverse relationship between the number of EPOR immunoreactive cells and the severity of ischaemic neuronal necrosis ($P = 0.040$) denotes outlying values in (B) and (E). In the box plots the median line is shown, the bar represents the upper 75% and lower 25% quartile, and the error bar depicts high and low values. (B, D–E). Necrosis scores represent the severity of nuclear changes characteristic of ischaemic neuronal necrosis ranging from areas with normal nuclear morphology (Score 0) to areas where most of the neurons are severely damaged (Score 4). For details see Materials and methods, Neuropathology.

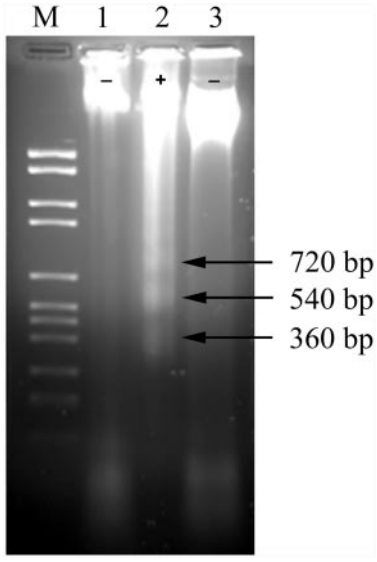

Fig. 4 DNA ladder. Agarose gel electrophoresis of DNA isolated from control tissues (lanes 1 and 3) and ischaemic brain tissue (lane 2). Lane identification: Lane M, the DNA size marker (fragment sizes from top to bottom: 2200, 1800, 1200, 1000, 650, 520, 450, 390, 300, 230, 220 and 150 bp); Lane 1, DNA isolated from the temporal lobe of control brain (autopsy delay 14 h); Lane 2, DNA isolated from the temporal lobe of ischaemic hemisphere of Case 9 (autopsy delay 4.5 h); Lane 3, DNA from the frontal lobe of a patient who died from basilar artery thrombosis (autopsy delay 13 h). + = DNA ladder is present, – = absent. Arrows on the right show multiples of 180 bp oligonucleosomal fragments resulting from apoptotic DNA fragmentation.

EPO and NF-200 in the double-labelling immunofluorescent staining (Fig. 5A and B). No statistically significant differences were detected between the mean number of EPO immunoperoxidase positive neuronal extensions in the controls and in post-ischaemic brains (n = 13). When a 4-scale grouping of the intensity of EPO immunoreactive signal was applied (0 = control level EPO immunoreactivity; + = faint immunoreactivity; ++ = moderate immunoreactivity; and +++ = strong immunoreactivity), all control brains showed low grade intensity i.e. Score 0. A major proportion of post-ischaemic sections fell into intensity groups exceeding this control level, i.e. only $\leq$30% of the cases showed control level EPO intensity, with the exception of ischaemic core region of the most acute cases (0.6–1.2 days; n = 3), in which two-thirds exhibited control level EPO-staining intensity. Most intense EPO immunoreactivity (+++) was evident in $\geq$30% of the sections in the infract core and periinfarct area after subacute and chronic ischaemia duration (1.6–18 days; n = 10).

Immunoreactivity for EPOR was strikingly absent in the control brains. Only scattered small- and large-sized cell somas and cellular extensions were EPOR immunoreactive. In the post-ischaemic brains, the generally more abundant EPOR immunoreactivity was detected to be concentrated in large cell somas. At day 1, somas of cells consistent with neuronal morphology showed bilateral EPOR immunoreactivity. Double-labelling immunofluorescence confirmed the neuronal dominance in the cellular EPOR immunoreactivity (Fig. 5C–E). Contralateral predominance of neuronal EPOR immunoreactivity in a location homologous to infarct core was evident during the post-ischaemic days 2–5 [106 (14) versus 2 (2) somas/mm^2 in the controls, $P < 0.05$]. Bilateral neuronal immunoreactivity for EPOR persisted up to a chronic stage of ischaemia. When co-registered with ischaemic neuronal necrosis, EPOR-immunoreactive cell somas decreased with increasing severity of ischaemic neuronal necrosis ($P = 0.040$) (Fig. 3E). The number of EPOR immunoreactive cell somas correlated with EPOR immunoreactive cellular extensions (Kendall's tau-b 0.220, $P = 0.047$).

Triple-labelling immunofluorescent staining of TUNEL with FasL, EPO or EPOR, and DAPI

Post-ischaemic FasL immunoreactivity colocalized with TUNEL-labelling (Fig. 2H). Only in rare occasions the TUNEL-labelled apoptotic cells also co-expressed EPO [2% (2); range 0–11% of all cells]; thus, cytoplasmic EPO immunofluorescence seemed to evade neuronal somas in which nuclear TUNEL-labelling was evident. Especially in the infarct core, EPO immunofluorescence in larger cell somas dissociated from TUNEL-labelling (Fig. 2F). Colocalization of cytoplasmic EPOR immunofluorescence with nuclear TUNEL-labelling was even more exceptional. Only 1% (1) of TUNEL-labelled apoptotic cells from the total (DAPI) number in both periinfarct and infarct core region co-expressed also EPOR.

Discussion

The main objective of this study was to describe the pattern of apoptotic cell damage in the course of ischaemic human stroke. The presence of apoptotic DNA fragmentation was also confirmed by DNA laddering and supported by expression of Fas–FasL, a dominant triggering system belonging to the TNF death receptor family inducing apoptotic cell death. Random necrotic DNA fragmentation was found in all studied ischaemic samples irrespective of the delay in autopsy, suggesting that both necrotic and apoptotic cell death is present in infarcted brains, whereas in non-ischaemic samples hardly any random or apoptotic DNA fragmentation is detectable. Furthermore, DNA laddering was negative in the brain specimens after death due to non-neurological causes and in the unaffected frontal lobe of a basilar artery thrombosis patient. Even though visualization of DNA ladder is difficult in tissue with concomitant ischaemic necrosis and post-mortem degradation, we consider it an important independent evidence of the presence of apoptotic cell death, since (i) the presence of the mononucleosomal and oligonucleosomal DNA fragments is a definitive marker of apoptosis (Earnshaw, 1995) and (ii) the presence of a visible DNA ladder

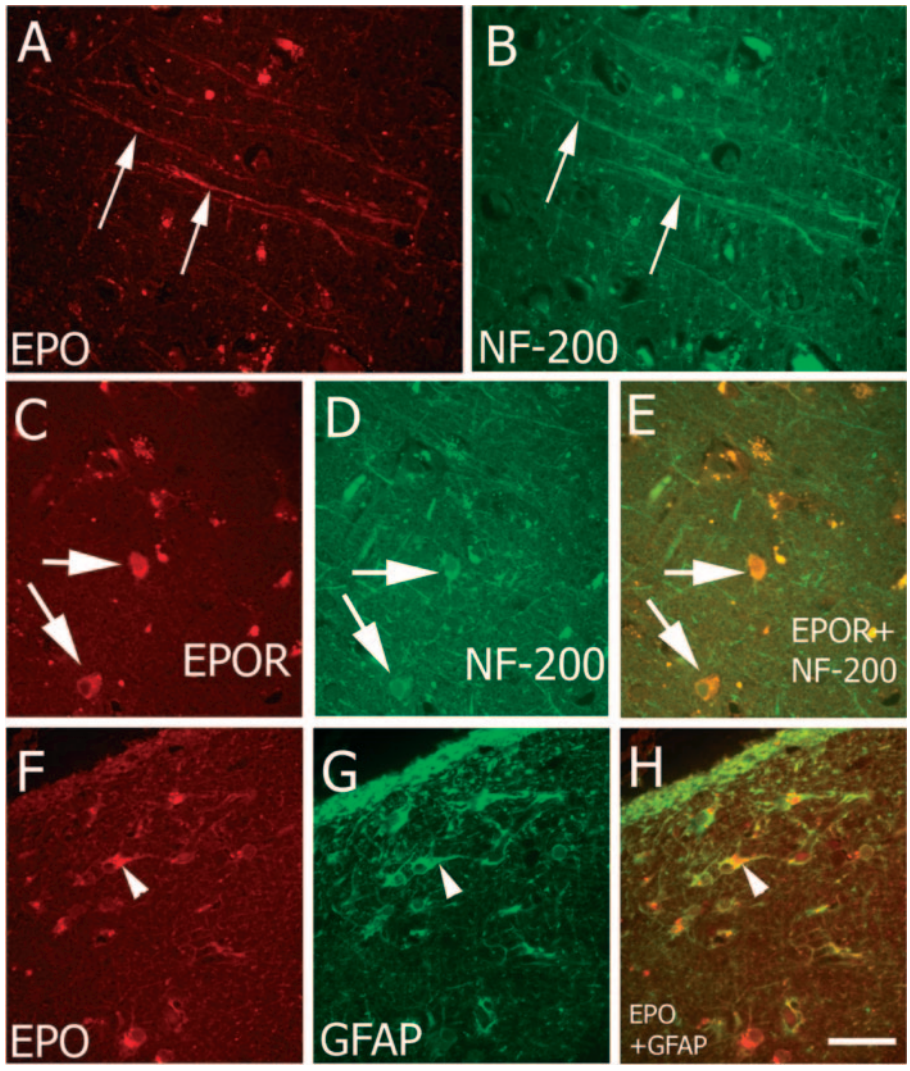

Fig. 5 Double-labelling immunofluorescent localization of EPO (**A**, **F** and **H**), EPOR (**C** and **E**) and cellular markers (**D–E** and **G–H**) in ischaemic human brain. (**A**) and (**B**), Neuronal origin of the majority of the EPO immunoreactive cells is confirmed by prominent overlap between EPO (A) and neurofilament immunofluorescence (B) (arrows). (**C–E**), The neuronal localization of EPOR is also evident by thorough colocalization of EPOR (C) and neurofilament (D) (arrows). (E) Orange colour depicts EPOR-expressing neurons in the periinfarct area at 2.5 days (arrows). (**F–H**), Glial EPO immunoreactivity became evident in post-ischaemic brains during the second day and bilateral glial EPO immunoreactivity peaked between days 2 and 5. The majority of EPO immunoreactive glia-like cells were confirmed to be astroglia by extensive colocalization of EPO (F) and GFAP (G) (arrow heads). (H), Orange colour depicts cytoplasmic EPO staining in an astrocyte (arrow head). Magnification ×300. Scale bar = 40 μm.

means that there is significant amount of apoptotic cell death in the tissue studied.

Our results are in line with the concept derived from studies on experimental brain ischaemia that apoptosis and necrosis are concurrent events after cerebral ischaemia (Hu *et al.*, 2002; Ünal-Çevik *et al.*, 2004). Their relative contribution to the total amount of cellular loss is dependent on the intensity of the ischaemic insult and the consequent availability of ATP as much as on the age and the context of the neuron (McManus and Buchan, 2000). Our results support the view that apoptosis is responsible for a minor proportion of cells lost in areas of deepest ischaemia, where necrosis is mostly responsible for cellular death, but the significance of apoptosis increases in brain areas with less severe acute ischaemic damage (Nicotera and Lipton, 1999). It has been suggested that necrosis would simply reflect the failure of neurons to perform the default programme of apoptotic cell death after cellular insult (Nicotera and Lipton, 1999), also when death receptor systems have been activated. Finally, as in experiments using ischaemic rat brain homogenates, the concomitance of apoptosis and necrosis, as evidenced by the nucleosomal ladder pattern superimposed on the smear of random DNA fragmentation (Hu *et al.*, 2002), was repeated in the present clinical material (Fig. 4).

Tissue richest in TUNEL-tagged cells with apoptotic morphology was found in brain areas outside the necrotic core (Fig. 3A), and this is supported by an inverse correlation between the severity of necrotic morphological cell changes

and the prevalence of TUNEL-labelled nuclei with apoptotic morphology (Fig. 3B). The decrease in TUNEL-labelled cells was concurrent with a decreasing number of FasL expressing cells in infarct areas with more advanced ischaemic necrotic changes. This indirectly suggests a role for FasL in fuelling post-ischaemic apoptotic neuronal cell damage in the periinfarct area. The periinfarct brain tissue represents a region where active programming of energy-dependent cell suicide is still ongoing during a prolonged time window. This area is at a risk of further neuronal cell drop-out through ischaemia-induced gene expression, which can potentially be corrected by putative 'rescue molecules or ligands' and gene-regulating treatments, including anti-apoptotic, such as anti-caspase, treatments (Onténiente *et al.*, 2003).

TUNEL-labelled neuronal cells that showed morphological changes towards loss of cellular integrity (i.e. thickening of the nuclear envelope and condensation of the chromatin) were detected also in the non-infarcted hemisphere. This is in line with the detection of TUNEL-labelled cells in normal rodent brains (Charriaut-Marlangue *et al.*, 1996; Chen *et al.*, 1997). The bilateral, 'basal' TUNEL-labelling may reflect an attempt towards cellular turnover serving organ integrity or plasticity processes in these aged brains as has been suggested for caspases (McLaughlin, 2004). Alternatively, it might represent consequences of cerebral herniation, which was found in five patients. But it was seen equally in non-herniated brains as well. We raise a possibility that it may reflect a kind of fatal transcallosal synaptic disconnection of neurons with their lifelong counterparts in the infarcted hemisphere that were faced with immediate necrotic cell death or imminent apoptosis. The loss of this vital neurotrophic input normally maintained by constant synaptic signalling may 'prime' the cells of the non-infarcted hemisphere to switch their gene expression towards plastic or regenerative changes, or perhaps promote a controlled non-inflammatory form of cell elimination in the circumstances of terminally disrupted neuronal networking. Finally, it has been suggested that in human lung epithelium, TUNEL-labelled cells with DNA damage may or may not proceed to apoptotic cell death (Liu *et al.*, 2005). Apoptotic pathways involving the cascade of intracellular caspase proteases may disrupt DNA repair mechanisms such as poly (ADP-ribose) polymerase (PARP) and thus serve as a point of no-return to repair of DNA damaged cells (Liu *et al.*, 2005). Thus it is our future interest to investigate the activation of caspases also in the hemisphere contralateral to ischaemia.

Post-ischaemic EPOR immunoreactivity appeared early (day 1), with contralateral hemispheric predominance, and the number of EPOR immunopositive neuronal somas peaked between days 2 and 5 as compared with the ischaemic hemisphere ($P < 0.05$). This may represent ischaemia-induced signalling towards cell survival-promoting gene regulation. Only scattered neuronal somas showed faint EPOR immunoreactivity in non-infarcted brains, confirming previous observation in rodents (Brines *et al.*, 2000). EPO immunoreactivity, on the other hand, was abundantly expressed in controls and the bilaterally observed post-ischaemic expression was concentrated in neuronal extensions, with no obvious increase in the number of EPO expressing neurons. The cellular localization of EPO in the neuronal extensions may reflect transport of the EPO-hormone to the synapse or intercellular space.

EPOR expression decreased as the degree of ischaemic neuronal necrosis increased (Fig. 3E), raising the possibility that in areas where apoptotic neuronal injury was imminent, neighbouring cells attempted to increase EPO-signalling. Indeed, the almost complete dissociation of EPO and EPOR with TUNEL-labelled cells (Fig. 2F) could reflect the lack of EPO-signalling in dying cells. Whether the lack of EPO expression is due to increased EPO consumption or depressed synthesis in the metabolically challenged milieu of the periinfarct area of the affected hemisphere cannot be addressed in the present study.

An attempt for survival and organ repair of the 'orphaned' neurons in the non-infarcted hemisphere might include increased expression of receptors mediating trophic signals such as EPOR. Similarly, in the periinfarct areas of the ipsilateral hemisphere marked by abundant EPOR expression, exogenously administered EPO might elicit EPO-signalling and promote cell survival. This is intriguing, as one blinded placebo-controlled pilot study has suggested a better clinical outcome at 1 month with EPO-treatment in acute stroke (Ehrenreich *et al.*, 2002), a finding awaiting replication in a large-scale clinical trial. Taken together, our results demonstrate apoptotic cell damage concomitantly with necrotic cell loss in human ischaemic stroke. The observation that apoptotic neuronal changes predominate in the infarct periphery support anti-apoptotic treatments to salvage brain tissue in danger of further cell death.

Acknowledgements

The study was financially supported by the Finnish Academy, Sigrid Jusélius Foundation, HUCH governmental subsidiary grants for research (EVO), Päivikki and Sakari Sohlberg Foundation, H. Lundbeck Inc. and Aarne Koskelo Foundation.

References

Agnello D, Bigini P, Villa P, Mennini T, Cerami A, Brines ML, et al. Erythropoietin exerts an anti-inflammatory effect on the CNS in a model of experimental autoimmune encephalomyelitis. Brain Res 2002; 952: 128–34.

Bernaudin M, Marti HH, Roussel S, Divoux D, Nouvelot A, MacKenzie ET, et al. A potential role for erythropoietin in focal permanent cerebral ischemia in mice. J Cereb Blood Flow Metab 1999; 19: 643–51.

Blin N, Stafford DW. A general method for isolation of high molecular weight DNA from eukaryotes. Nucleic Acids Res 1976; 3: 2303–08.

Brines ML, Ghezzi P, Keenan S, Agnello D, de Lanerolle NC, Cerami C, et al. Erythropoietin crosses the blood-brain barrier to protect against experimental brain injury. Proc Natl Acad Sci USA 2000; 97: 10526–31.

Cattaneo E, De Fraja C, Conti L, Reinach B, Bolis L, Govoni S, et al. Activation of the JAK/STAT pathway leads to proliferation of ST14A central nervous system progenitor cells. J Biol Chem 1996; 271: 23374–9.

Charriaut-Marlangue C, Margaill I, Popovici T, Plotkine M, Ben-Ari Y. Apoptosis and necrosis after reversible focal ischemia: an in situ DNA fragmentation analysis. J Cereb Blood Flow Metab 1996; 16: 186–94.

Chen J, Jin K, Chen M, Pei W, Kawaguchi K, Greenberg DA, et al. Early detection of DNA strand breaks in the brain after transient focal ischemia: implications for the role of DNA damage in apoptosis and neuronal death. J Neurochemistry 1997; 69: 232–45.

Conrad KP, Benyo DF, Westerhausen-Larsen A, Miles TM. Expression of erythropoietin by the human placenta. FASEB J 1996; 10: 760–6.

Digicaylioglu M, Bichet S, Marti HH, Wenger RH, Rivas LA, Bauer C, et al. Localization of specific erythropoietin binding sites in defined areas of the mouse brain. Proc Natl Acad Sci USA 1995; 92: 3717–20.

Earnshaw WC. Nuclear changes in apoptosis. Curr Biol 1995; 7: 337–43.

Ehrenreich H, Hasselblatt M, Dembowski C, Cepek L, Lewczuk P, Stiefel M, et al. Erythropoietin therapy for acute stroke is both safe and beneficial. Mol Med 2002; 8: 495–505.

Eke A, Conger KA, Anderson M, Garcia JH. Histologic assessment of neurons in rat models of cerebral ischemia. Stroke 1990; 21: 299–304.

Guglielmo MA, Chan PT, Cortez S, Stopa EG, McMillan P, Johanson CE, et al. The temporal profile and morphological features of neuronal death in human stroke resemble those observed in experimental forebrain ischemia: The potential role of apoptosis. Neurol Res 1998; 20: 283–96.

Hu X, Johansson I-M, Brännström T, Olsson T, Wester P. Long-lasting neuronal apoptotic cell death in regions with severe ischemia after photothrombotic ring stroke in rats. Acta Neuropathol 2002; 104: 462–70.

Lindsberg PJ, Carpen O, Paetau A, Karjalainen-Lindsberg M-L, Kaste M. Endothelial ICAM-1 expression associated with inflammatory cell response in human ischemic stroke. Circulation 1996; 94: 939–45.

Liu X, Conner H, Kobayashi T, Kim H, Wen F, Abe S, et al. Cigarette smoke extract induces DNA damage but not apoptosis in human bronchial epithelial cells. Am J Respir Cell Mol Biol 2005; 33: 121–9.

Love S, Barber R, Wilcock GK. Neuronal death in brain infarcts in man. Neuropathol Appl Neurobiol 2000; 26: 55–66.

McLaughlin B. The kinder side of killer proteases: caspase activation contributes to neuroprotection and CNS remodeling. Apoptosis 2004; 9: 111–21.

McManus JP, Buchan AM. Apoptosis after experimental stroke; fact or fashion? J Neurotrauma 2000; 17: 899–914.

Morishita E, Masuda S, Nagao M, Yasuda Y, Sasaki R. Erythropoietin receptor is expressed in rat hippocampal and cerebral cortical neurons, and erythropoietin prevents in vitro glutamate-induced neuronal death. Neuroscience 1997; 76: 105–16.

Moritz KM, Lim GB, Wintour EM. Developmental regulation of erythropoietin and erythropoiesis. Am J Physiol 1997; 273: R1829–44.

Nicotera P, Lipton SA. Excitotoxins in neuronal apoptosis and necrosis. J Cereb Blood Flow Metab 1999; 19: 583–91.

O'Connell J, Houston A, Bennett MW, O'Sullivan GC, Shanahan F. Immune privilege or inflammation? Insights into the Fas ligand enigma. Nature Med 2001; 7: 271–274.

Onténiente B, Cuoriaud C, Braudeau J, Benchoua A, Guegan C. The mechanisms of cell death in focal cerebral ischemia highlight neuroprotective perspectives by anti-caspase therapy. Biochem Pharmacol 2003; 66: 1634–49.

Sadamoto Y, Igase K, Sakanaka M, Sato K, Otsuka H, Sakaki S, et al. Erythropoietin prevents place navigation disability and cortical infarction in rats with permanent occlusion of the middle cerebral artery. Biochem Biophys Res Commun 1998; 253: 26–32.

Sairanen T, Ristimäki A, Karjalainen-Lindsberg M-L, Paetau A, Kaste M, Lindsberg PJ. Cyclooxygenase-2 is induced globally in infarcted human brain. Ann Neurol 1998; 43: 738–47.

Sairanen T, Carpen O, Karjalainen-Lindsberg M-L, Paetau A, Turpeinen U, Kaste M, et al. Evolution of cerebral tumor necrosis factor-α production during human ischemic stroke. Stroke 2001; 32: 1750–58.

Sakanaka M, Wen TC, Matsuda S, Masuda S, Morishita E, Nagao M, et al. In vivo evidence that erythropoietin protects neurons from ischemic damage. Proc Natl Acad Sci USA 1998; 95: 4635–4640.

Semenza GL, Wang GL. A nuclear factor induced by hypoxia via de novo protein synthesis binds to the human erythropoietin gene enhancer at a site required for transcriptional activation. Mol Cell Biol 1992; 12: 5447–54.

Sharma K, Wang RX, Zhang LY, Yin DL, Luo XY, Solomon JC, et al. Death the Fas way: regulation and pathophysiology of CD95 and its ligand. Pharmacol Ther 2000; 88: 333–47.

Siren A-L, Fratelli M, Brines M, Goemans C, Casagrande S, Lewczuk P, et al. Erythropoietin prevents neuronal apoptosis after cerebral ischemia and metabolic stress. Proc Natl Acad Sci USA 2001; 98: 4044–9.

Stähelin BJ, Marti U, Solioz M, Zimmermann H, Reichen J. False positive staining in the TUNEL assay to detect apoptosis in liver and intestine is caused by endogenous nucleases and inhibited by diethyl pyrocarbonate. J Clin Pathol 1998; 51: 204–8.

Ünal-Çevik I, Kilinç M, Can A, Gürsoy-Özdemir Y, Dalkara T. Apoptotic and necrotic death mechanisms are concomitantly activated in the same cell after cerebral ischemia. Stroke 2004; 35: 2189–94.

Yoshimura A, Misawa H. Physiology and function of the erythropoietin receptor. Curr Opin Hematol 1998; 5: 171–6.